AJNR

Assessment of Collateral Flow in Patients with Carotid Stenosis Using Random Vessel-Encoded Arterial Spin-Labeling: Comparison with Digital Subtraction Angiography

Shanshan Lu, Chunqiu Su, Yuezhou Cao, Zhenyu Jia, Haibin Shi, Yining He and Lirong Yan

This information is current as of June 29, 2025.

AJNR Am J Neuroradiol 2024, 45 (2) 155-162
doi: https://doi.org/10.3174/ajnr.A8100
http://www.ajnr.org/content/45/2/155

Assessment of Collateral Flow in Patients with Carotid Stenosis Using Random Vessel-Encoded Arterial Spin-Labeling: Comparison with Digital Subtraction Angiography

Shanshan Lu, Chunqiu Su, Yuezhou Cao, Zhenyu Jia, Haibin Shi, Yining He, and Lirong Yan

ABSTRACT

BACKGROUND AND PURPOSE: Collateral circulation plays an important role in steno-occlusive internal carotid artery disease (ICAD) to reduce the risk of stroke. We aimed to investigate the utility of planning-free random vessel-encoded arterial spin-labeling (rVE-ASL) in assessing collateral flows in patients with ICAD.

MATERIALS AND METHODS: Forty patients with ICAD were prospectively recruited. The presence and extent of collateral flow were assessed and compared between rVE-ASL and DSA by using Contingency (C) and Cramer V (V) coefficients. The differences in flow territory alterations stratified by stenosis ratio and symptoms, respectively, were compared between symptomatic ($n = 19$) and asymptomatic ($n = 21$) patients by using the Fisher exact test.

RESULTS: Good agreement was observed between rVE-ASL and DSA in assessing collateral flow (C = 0.762, V = 0.833, both $P < .001$). Patients with ICA stenosis of ≥90% were more likely to have flow alterations ($P < .001$). Symptomatic patients showed a higher prevalence of flow alterations in the territory of the MCA on the same side of ICAD (63.2%), compared with asymptomatic patients (23.8%, $P = .012$), while the flow alterations in the territory of anterior cerebral artery did not differ ($P = .442$). The collateral flow to MCA territory was developed primarily from the contralateral internal carotid artery (70.6%) and vertebrobasilar artery to a lesser extent (47.1%).

CONCLUSIONS: rVE-ASL provides comparable information with DSA on the assessment of collateral flow. The flow alterations in the MCA territory may be attributed to symptomatic ICAD.

ABBREVIATIONS: ACA = anterior cerebral artery; AcomA = anterior communicating artery; ASL = arterial spin-labeling; ECA = external carotid artery; ICAD = internal carotid artery disease; pCASL = pseudocontinuous ASL; PcomA = posterior communicating artery; rVE-ASL = random vessel-encoded arterial spin-labeling; SS = super-selective; VBA = vertebrobasilar artery; VE = vessel-encoded

Collateral circulation plays a pivotal role in maintaining cerebral perfusion, metabolism, and function in patients with steno-occlusive internal carotid artery disease (ICAD).[1] The overall annual risk of stroke is ~9%–18% in symptomatic patients with ICAD with compromised cerebral perfusion and poor collateral flow.[2] Adequate collateral circulation can prevent hemodynamic deterioration and lower the risk of stroke occurrence.[2,3] The primary collateral flow develops in the circle of Willis via the anterior and posterior communicating arteries (AcomA and PcomA, respectively). Secondary collateral pathways include the external carotid artery (ECA) via the ophthalmic artery and leptomeningeal anastomoses at the brain surface, which are recruited when the primary collaterals are insufficient.[4] In clinical practice, DSA remains the reference standard to assess collateral circulations. However, this procedure is invasive and bears the risk of neurologic complications and ionizing radiation, limiting its availability for routine long-term surveillance.[5,6] A noninvasive method that demonstrates selective angiographic information is desired to investigate collateral blood flow.

Arterial spin-labeling (ASL) MR perfusion imaging offers a noninvasive approach to measuring cerebral perfusion.[7-10] Among the ASL variants, vessel-selective ASL techniques enable depicting flow territories and assessing collateral pathways, where an individual or groups of brain-feeding arteries are labeled.[2,11-15] Super-selective ASL (SS-ASL) and vessel-encoded ASL (VE-ASL) are 2 conventional vessel-selective ASL techniques that are based on pseudocontinuous ASL (pCASL) but employ additional

Received July 12, 2023; accepted after revision November 7.

From the Departments of Radiology (S.L., C.S.) and Interventional Radiology (Y.C., Z.J., H.S.), The First Affiliated Hospital of Nanjing Medical University, Nanjing, Jiangsu Province, China; and Department of Radiology (Y.H., L.Y.), Feinberg School of Medicine, Northwestern University, Chicago, Illinois.

S. Lu and C. Su contributed equally to this work.

Please address correspondence to Lirong Yan, Department of Radiology, Feinberg School of Medicine, Northwestern University, 737 N Michigan Ave, Suite 1600, Chicago, IL 60611; e-mail: lirong.yan@northwestern.edu

Indicates article with online supplemental data.

http://dx.doi.org/10.3174/ajnr.A8100

gradients in between the radiofrequency pulses.[14-16] SS-ASL enables the labeling of a single artery,[14,15] while VE-ASL can label multiple vessels simultaneously.[16] However, prior knowledge of the positions of the feeding arteries is required during the implementation of both SS-ASL and VE-ASL, which increases the complexity of the protocol setting and prolongs scan preparation time.[12] Furthermore, these conventional vessel-selective ASL techniques are vulnerable to field inhomogeneity at the labeling locations.[17,18] To address the limitations, a random VE-ASL (rVE-ASL) has been introduced,[13] which not only allows for mapping vascular territories without prior knowledge but also uniquely identifies the locations of the corresponding feeding arteries in the tagging plane.

In this study, we aimed to evaluate the clinical utility of rVE-ASL in assessing collateral flows by comparison with DSA as the reference standard in patients with ICAD. We further investigated the flow alterations between patients with symptomatic and asymptomatic ICAD.

MATERIALS AND METHODS

Patients

The ethics committee of our institution approved the study protocol, and written informed consent was obtained from all patients. From February 2018 to December 2021, we recruited 53 patients with ICAD presenting with ICA stenosis (≥50%) or occlusion on noninvasive imaging (CT angiography, MR angiography, or ultrasonography) who underwent DSA for further evaluation and agreed to participate in rVE-ASL imaging from our single center. Those patients either experienced recent neurologic events (acute ischemic stroke or transient ischemic attack) or nonspecific neurologic symptoms, such as dizziness and headache. For patients with nonspecific symptoms, DSA was considered by clinicians for further evaluation when patients presented with ICA stenosis of ≥70%, or with ICA stenosis of ≥50% and had unstable plaques on noninvasive images. The time interval between DSA and rVE-ASL was within 1 week. After imaging, those with severe motion artifacts ($n = 8$) on rVE-ASL, bilateral ICA stenosis ($n = 3$), or severe intracranial arterial stenosis ($n = 2$) were excluded from further analyses. Finally, 40 patients (34 men, mean age 68.0 ± 10.8 years) were enrolled, including 19 symptomatic patients and 21 asymptomatic patients.

MR Imaging Protocol

All the experiments were performed on a 3T MR scanner (Magnetom Skyra, Siemens) by using a 20-channel head-neck coil. Compressed-sensing time-of-flight MRA (CS TOF-MRA) equipped with inline reconstruction was performed with the following parameters:[19] TR = 21 ms, TE = 3.49 ms, flip angle = 18°, FOV = 220 × 200 mm^2, matrix = 368 × 334, acquired resolution = 0.6 × 0.6 × 0.6 mm^3, and reconstructed resolution = 0.4 × 0.4 × 0.4 mm^3. The TOF coverage extended from the bifurcation of the common carotid artery to the body of the corpus callosum (16 cm). DWI was performed with the imaging parameters as follows: b-value = 1000 mm^2/s, TR = 6400 ms, TE = 98 ms, FOV = 220 × 220 mm^2, matrix = 192 × 192, section thickness = 4 mm, 20 slices. T2-weighted FLAIR was performed with the following parameters: TR = 8000 ms, TE = 97 ms, TI = 2370 ms, FOV = 230 × 230 mm^2, matrix = 256 × 230, section thickness = 5 mm, 20 slices.

rVE-ASL scan with background suppressed single-shot 3D gradient- and spin-echo acquisition was performed with the following parameters: FOV = 220 × 220 mm^2, matrix = 64 × 64, TR = 3650 ms, TE = 36 ms, labeling duration = 1500 ms, post-labeling delay = 1500 ms, 12 slices with the section thickness of 8 mm, 60 pairs of encoding steps with random orientation, phase and wavelength were acquired with 2 additional pairs of global label/control, leading to a total scan time of 7 minutes 32 seconds.

Table 1: Distribution of collaterals grades by rVE-ASL and DSA

rVE-ASL collateral grade	DSA collateral grade				Total
	0	1	2	3	
0	0	0	0	0	0
1	0	12	2	0	14
2	0	1	4	0	5
3	0	0	0	21	21
Total	0	13	6	21	40

Note:— 0: poor, no visible collaterals; 1: intermediate, partial collateral flow to the side of stenosis/occlusion; 2: good, full collateral flow to the side of stenosis/occlusion; 3: normal antegrade flow.

DSA Protocol

DSA was performed by using the modified Seldinger method with a DSA machine (Allura Xper FD20, Philips). A 5F headhunter catheter was introduced into the ascending aorta via the transfemoral route and navigated into the appropriate carotid or vertebral artery, as decided by the angiographer. The arteries were displayed in at least 2 projections by automatic injection of 6–8 mL of iodixanol 320 (Visipaque, GE Healthcare). DSA was performed with a 270-mm FOV and a 1024 matrix, yielding a measured pixel size of 0.27 × 0.27 mm^2. We used variable frames-per-second (fps) in the DSA protocol containing 3 phases (phase 1: 6 fps for 4 s; phase 2: 2 fps for 8 s; phase 3: 1 fps for the remaining acquisition).

rVE-ASL Postprocessing

rVE-ASL analysis was performed in MATLAB (MathWorks). The images were subtracted pair-wise, resulting in 60 vessel-encoded perfusion maps and 2 global perfusion maps. Theoretical ASL signals at each location in the labeling plane were calculated by using the 60 sets of predefined encoding parameters. The locations of feeding arteries were identified by calculating the correlation coefficient between the acquired perfusion signal per voxel and the theoretical ASL signals, and the corresponding perfusion territorial maps were subsequently determined based on the maximum correlation coefficient of each voxel. We divided the perfusion territories into 3 regions: right ICA, left ICA, and vertebrobasilar artery (VBA) territories. These images were subsequently combined into a red-green-blue frame to demonstrate the spatial distribution of the 3 perfusion territories (right ICA territory as green, left ICA territory as red, and VBA territory as blue).

Assessment of ICA Stenosis and Collateral Flow

The luminal stenosis ratio was calculated by 1 experienced neurointerventional radiologist (14 years of experience) on DSA

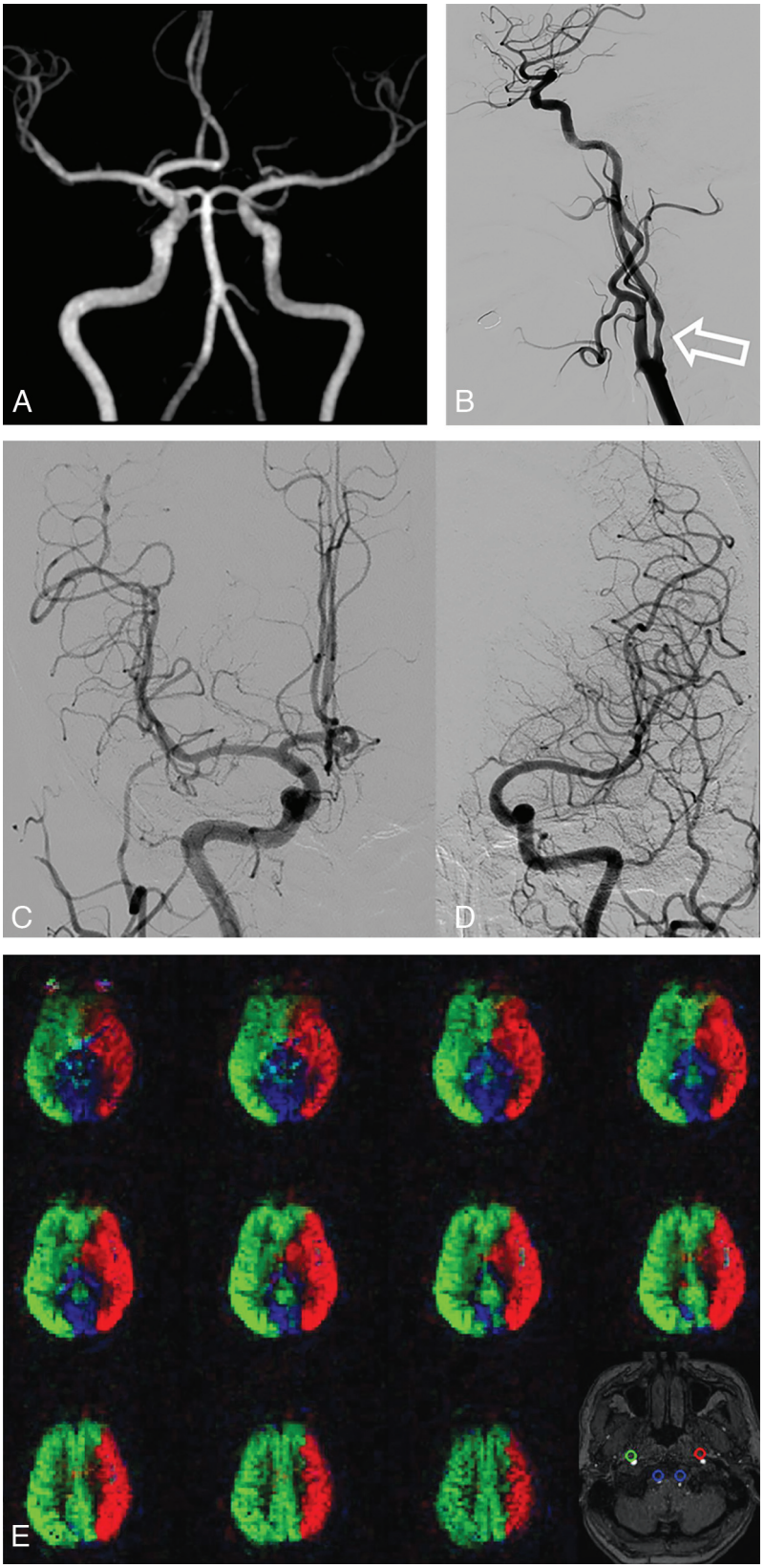

FIG 1. A 71-year-old male asymptomatic patient with left ICA stenosis. *A*, TOF-MRA shows the absence of the left A1 segment of the circle of Willis in this patient. *B–D*, DSA reveals a left ICA stenosis of 60%, but with a normal antegrade flow (grade III). The right ICA angiogram reveals normal antegrade flow to the left ACA territory. *E*, Vascular territory maps generated by rVE-ASL display flow territories of left ICA (*red*), right ICA (*green*), and VBA (*blue*), along with detected feeding arteries on the labeling plane. The right ICA supplies the left ACA territory, consistent with the findings on DSA.

according to the North American Symptomatic Carotid Endarterectomy Trial method:[20] stenosis ratio (%) = (1 – artery diameter at the narrowest site/normal vessel diameter at the distal end of stenosis) × 100%. If there were multiple stenoses in 1 segment, only the most stenotic site was selected for calculation.

The presence of collateral flow was assessed with reference to a previous report:[21] 1) anterior collateral flow: from the normal side across the AcomA to the A2 segment on the side of ICAD only or flow from the normal side across the AcomA and retrograde flow in the A1 segment on the steno-occluded side that supplies both the A2 segment and the MCA on the side of the ICAD; 2) posterior collateral flow: from the PcomA that supplies the vascular territory of MCA on the side of the ICAD; and 3) collateral flow in the leptomeningeal anastomoses was considered to be present if DSA showed cortical branches extending from the posterior cerebral artery or anterior cerebral artery (ACA) into the vascular territory of the MCA. It is worth noting that any changes in flow territories caused by normal anatomic variants of the circle of Willis, such as hypoplasia/absent A1 segment or fetal origin of posterior cerebral artery, were not considered as the presence of collateral flow in this study. However, in cases where there was no variation in ACA (hypoplasia/absent A1 segment), flow from the contralateral side passing through the AcomA to reach the A2 segment on the side of ICAD was considered as anterior collateral flow.

The extent of collateral flow was graded on both rVE-ASL and DSA at the ipsilateral hemisphere to the ICAD for each patient, respectively, giving a total of 40 hemispheres. Two neuroradiologists (10 and 6 years of experience, respectively) and 2 neurointerventional radiologists (14 and 8 years of experience, respectively) independently assessed the collateral grades, according to the following scale: 0: poor, no visible collaterals; 1: intermediate, partial collateral flow to the side of ICAD; 2: good, full collateral flow to the side of ICAD; 3: normal antegrade flow. Any

Table 2: Flow alterations on rVE-ASL stratified by stenosis ratio

	Stenosis Ratio	With Flow Alterations, *n* (%)	Without Flow Alterations, *n* (%)	*P* Value
Flow territory of MCA on the side of ICAD	< 90% (*n* = 24)	2 (8.3)	22 (91.7)	<.001
	≥ 90% (*n* = 16)	15 (93.8)	1 (6.2)	
Flow territory of ACA on the side of ICAD	< 90% (*n* = 24)	0 (0.0)	24 (100.0)	<.001
	≥ 90% (*n* = 16)	8 (50.0)	8 (50.0)	

Table 3: Flow alterations on rVE-ASL stratified by symptoms

	Patient Group	With Flow Alterations, *n* (%)	Without Flow Alterations, *n* (%)	*P* Value
Flow territory of MCA on the side of ICAD	Symptomatic (*n* = 19)	12 (63.2)	7 (36.8)	.012
	Asymptomatic (*n* = 21)	5 (23.8)	16 (76.2)	
Flow territory of ACA on the side of ICAD	Symptomatic (*n* = 19)	5 (26.3)	14 (73.7)	.442
	Asymptomatic (*n* = 21)	3 (14.3)	18 (85.7)	

disagreement between the readers was solved by another senior neuroradiologist (28 years of experience).

Statistical Analysis

Quantitative data conforming to a normal distribution were represented as the mean ± SD; otherwise, as the median (interquartile range presented as the 25th and 75th percentiles). Categoric data were recorded as counts and percentages. Cohen kappa coefficient was calculated to evaluate the interobserver reliability for assessing the extent of collaterals on rVE-ASL and DSA. Contingency (C) and Cramer V (V) coefficients were calculated with χ^2 statistics and were used to compare the collateral grades between rVE-ASL and DSA. The difference in flow alterations between symptomatic and asymptomatic patients was assessed by using the Fisher exact test. The *P* value was 2-sided, and $P < .05$ was considered statistically significant. All statistical analyses were conducted by using SPSS 22.0 (IBM).

RESULTS

Patient Characteristics

Of the 40 patients, 35 presented with ICA stenosis of 50%–99% and 5 presented with ICA occlusion. Anatomic variations of the circle of Willis were observed in 26 patients, including 16 patients with hypoplasia or absent A1 segment, 7 patients with fetal posterior cerebral artery, and 3 patients with both. The demographic, clinical, and imaging characteristics of patients are detailed in Online Supplemental Data.

Comparison of Collateral Grades between rVE-ASL and DSA

The interreader agreement in grading collaterals by using rVE-ASL and DSA was found to be good to excellent, with kappa values of 0.876 and 0.764, respectively. Good agreement was achieved between rVE-ASL and DSA in grading collateral flow ($C = 0.762$; $V = 0.833$; $P < .001$). Of the 40 patients, only 2 cases that were graded as collateral grade II on DSA were misclassified as grade I on rVE-ASL, and 1 case showing grade I collaterals on DSA was classified as grade II on rVE-ASL. For the remaining 37 cases, the collaterals revealed by rVE-ASL match completely with the findings from DSA (Table 1). Figure 1 shows an example of the vascular territory maps revealed by rVE-ASL from an asymptomatic patient with left ICA stenosis of 60%, where a normal antegrade flow was observed, consistent with the DSA findings.

Flow Alterations on rVE-ASL Stratified by Stenosis Ratio and Symptoms

Flow alterations were observed in 17 patients in the territory of MCA and 8 patients in the territory of ACA, respectively, on the side affected by ICAD (Online Supplemental Data). Notably, these flow alterations were more frequently observed in patients with high-grade ICA stenosis (≥90%) compared with those with <90% ICA stenosis, in both MCA and ACA vascular territories ($P < .001$ for both territories), as indicated in Table 2.

Symptomatic patients exhibited a high prevalence of flow alterations (63.2%) in the territory of MCA ipsilateral to ICAD, compared with asymptomatic patients (23.8%) ($P = .012$, as shown in Table 3). The collateral flow was primarily developed from the contralateral ICA via AcomA in 12 of 17 (70.6%) patients and from VBA via PcomA in 8 of 17 (47.1%) patients. Detailed information can be found in Online Supplemental Data. However, there were no significant differences in flow alterations in the territory of ACA between symptomatic and asymptomatic patients ($P = .442$). Figure 2 shows an example of an asymptomatic patient with right-side high-grade ICA stenosis. rVE-ASL demonstrated flow alterations in the territory of MCA with collaterals from the VBA, which was confirmed by DSA. Figure 3 shows a symptomatic case of ICAD with right ICA occlusion. Evident flow alterations in the territory of the right MCA with collaterals from the left ICA and the VBA were observed on rVE-ASL, consistent with DSA findings.

DISCUSSION

In this study, we successfully demonstrated the feasibility of using rVE-ASL to assess collateral flows in patients with ICAD. Our results showed a good to excellent agreement between rVE-ASL and the reference standard of DSA in determining the presence and the extent of collaterals. Patients with a severe grade of ICA stenosis (≥90%) were more prone to experiencing flow alterations. The presence of flow alterations in the territory of the MCA may be linked to symptomatic ICAD.

The ability to determine the arterial source of blood supply to specific brain regions or lesions is crucial for the clinical evaluation and treatment of patients with ICAD. Some noninvasive methods, such as dynamic contrast-enhanced MRA, 4D flow MR imaging, or MR perfusion, can be considered to evaluate

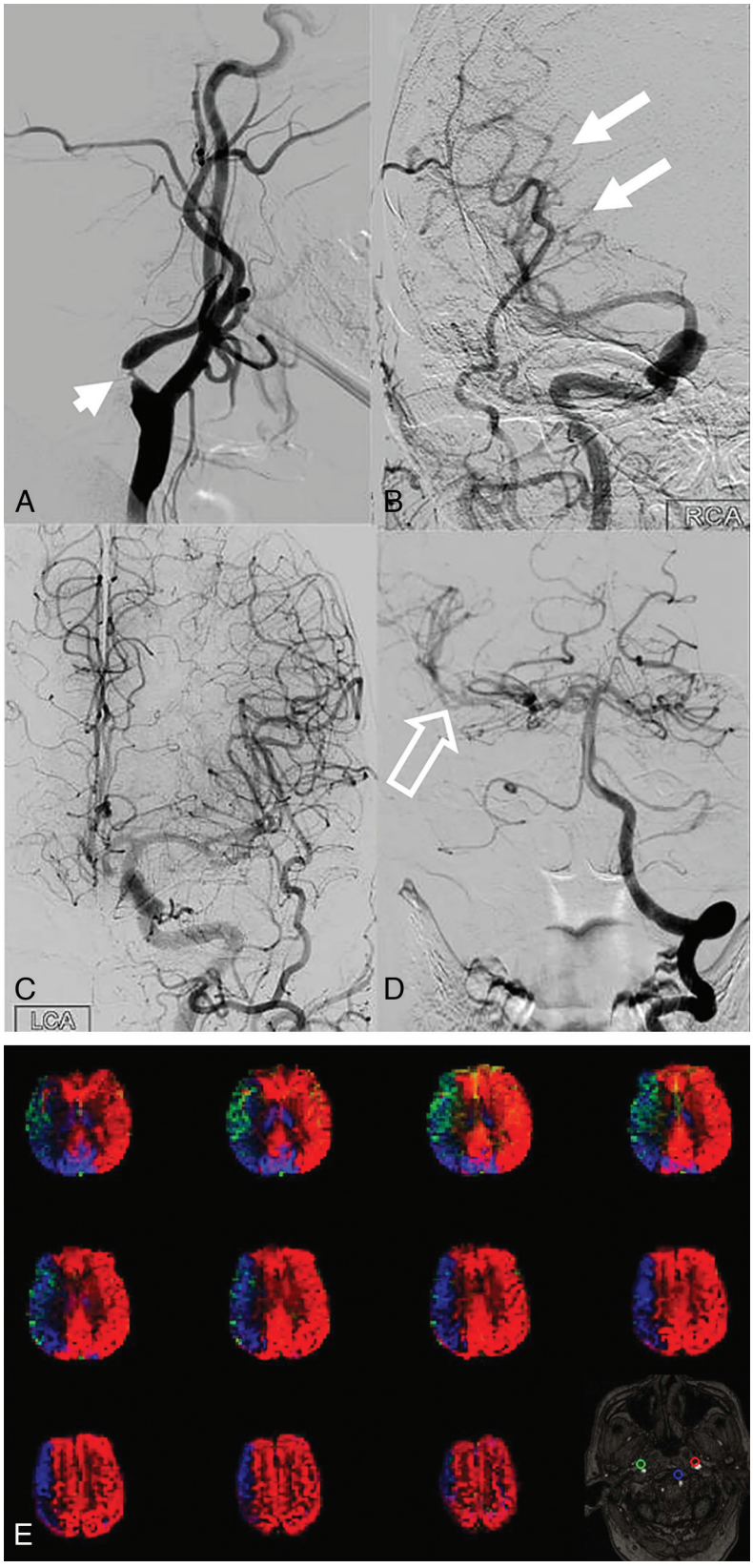

FIG 2. An 81-year-old male patient with dizziness for 2 years. *A–D*, DSA images reveal a very high-grade stenosis of the right ICA indicated by the white short arrow. The right ICA angiogram shows decreased flow to the right MCA territory (*white arrows*). The VBA angiogram shows significant collateral flow to the right MCA territory (*white hollow arrow*). The extent of collaterals is classified as grade I. *E*, Evident flow alterations are shown on vascular territory maps generated by rVE-ASL. The territory of right MCA is supplied by the right ICA (*green*) and VBA (*blue*), while the territory of right ACA is supplied by left ICA (*red*), consistent with the DSA findings. The extent of collaterals is also classified as grade I on rVE-ASL. The locations of the detected feeding arteries are shown in the bottom right of figure (*E*).

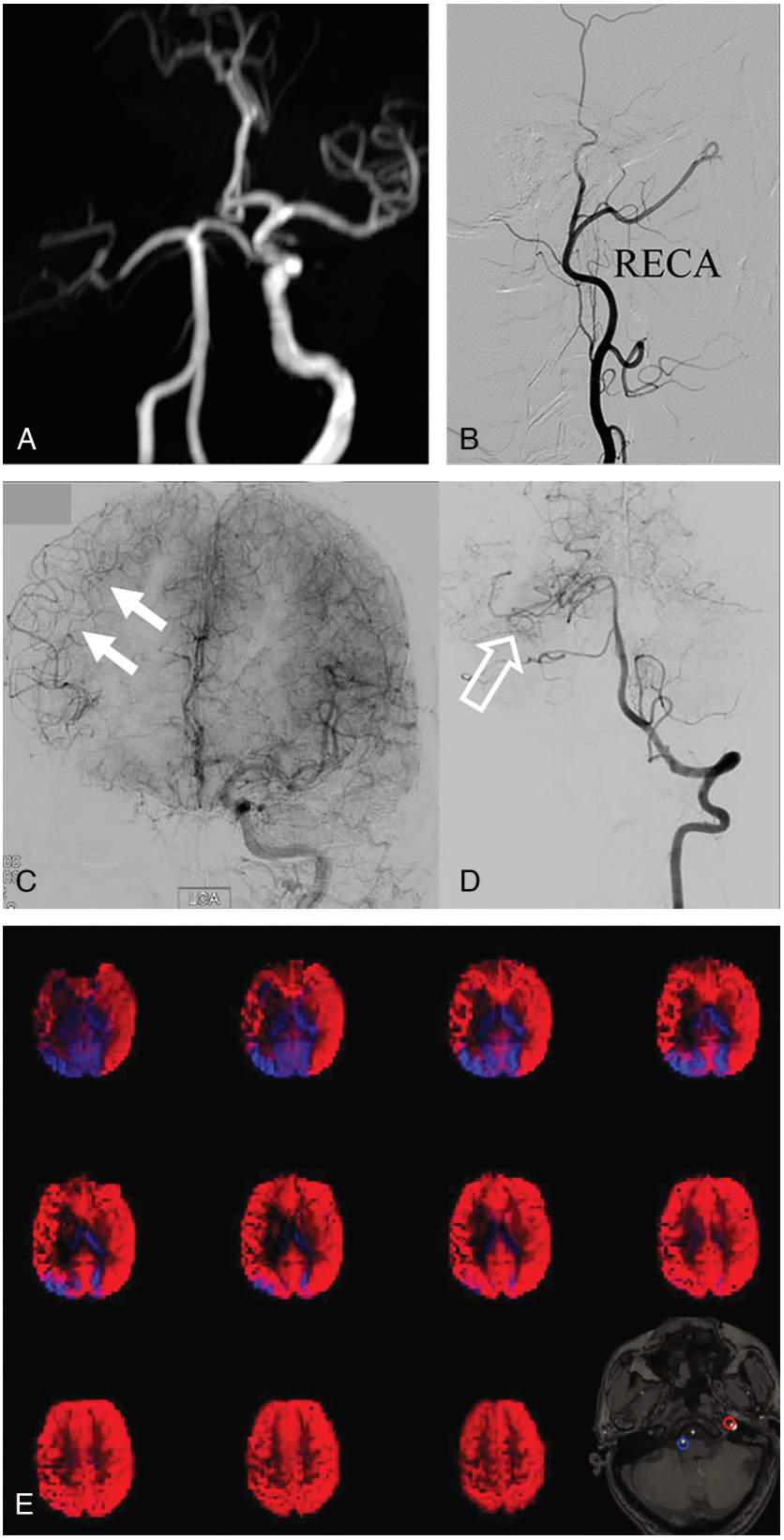

FIG 3. A 60-year-old man with left limb weakness for 3 days. *A*, TOF-MRA shows the occlusion in the right ICA and the absence of the right A1 segment of the circle of Willis in this patient. *B–D*, DSA confirms the occlusion of the right ICA, and the extent of collaterals is classified as grade I. The left ICA angiogram shows collateral flow to the right ACA and MCA territory via the AcomA and the leptomeningeal anastomoses (*white arrows*). The VBA angiogram shows collateral flow to the right MCA territory via the PcomA and leptomeningeal anastomoses (*white hollow arrow*). *E*, Vascular territory maps of rVE-ASL show flow territories of left ICA (*red*) and VBA (*blue*), while the flow territory of the right ICA (*green*) is absent. The territory of right MCA is mainly supplied by the left ICA, followed by VBA, consistent with the findings on DSA. The extent of collaterals is also classified as grade I on rVE-ASL. The locations of the detected feeding arteries are shown in the bottom right of figure (*E*).

patients with ICAD in clinical practice. Dynamic contrast-enhanced MRA and 4D flow MR imaging are considered "lumenography" and focus on depiction of dynamic blood flow patterns or measuring blood flow velocities in the cerebral vasculature. MR perfusion techniques, such as dynamic susceptibility contrast and conventional ASL, allow for CBF imaging. However, these MR imaging techniques can not characterize the collateral flow territories. Previous studies have suggested that vessel-selective ASL, such as VE-ASL and SS-ASL, could be a valuable tool for mapping the territories of main brain feeding arteries.[7,22-24] However, the conventional vessel-selective ASL techniques require prior knowledge of the locations of vessels to be tagged.[12,17,18] This in turn necessitates a collection of an angiogram and expertise in planning. In contrast, the rVE-ASL used in our study cannot only map vascular territories without the need for explicit planning but also identify the locations of corresponding source arteries in the tagging plane. This simplifies the scan procedure similar to conventional pCASL. In the conventional vessel-selective ASL based on pCASL, potential off-resonance at the locations of the arteries in the tagging plane can significantly impact the tagging efficiency. In contrast, rVE-ASL is insensitive to off-resonance effects similar to multiphase pseudocontinuous ASL.[13] Our study demonstrated a high consistency between vascular territory mapping by using rVE-ASL and DSA, indicating that rVE-ASL could serve as an alternative and noninvasive method to evaluate individual collateral pathways in patients with ICAD.

In this study, we observed that symptomatic patients with ICAD had a higher prevalence of flow alterations in the MCA territory on the affected side, compared with asymptomatic patients. However, there was no significant difference found in flow alterations in the ACA territory between symptomatic and asymptomatic patients. These findings are consistent with a previous study by van Laar et al,[21] which reported significant differences in the flow territories of the contralateral ICA and VBA in patients with symptomatic ICA occlusion compared with those in control subjects. They also reported that the MCA territory ipsilateral to the occluded ICA was primarily supplied by the VBA, whereas the flow territory of ACA on the occluded side was mainly supplied by the contralateral ICA. However, in contrast to their findings, our study found that collateral flow to the MCA territory on the side of ICAD was primarily developed from the contralateral ICA (70.6% via AcomA) and, to a lesser extent, from the VBA (47.1% via PcomA). These differences in the collateral flow patterns may be attributed to variations in the circle of Willis among individuals. Previous studies have also emphasized the importance of collateral flow from the contralateral ICA via AcomA or VBA.[25-29] Our results further support the significance of collateral flows from the contralateral ICA in maintaining blood flow in the MCA territory on the side of ICAD. In symptomatic patients without flow alteration, inadequate collateral compensation may lead to a borderzone infarct. Additionally, artery-to-artery embolism induced by vulnerable plaque can also contribute to the occurrence of stroke/TIA in these patients.

Our study also revealed a significant association between flow alterations and the degree of stenosis. Consistent with the findings of Chen et al,[30] who reported the existence of high-grade stenosis associated with hemispheric asymmetry in flow territory map, we found that a high-grade ICA stenosis (≥90%) was most likely to result in flow alterations. Traditionally, the stenotic rate of ICA ≥70% is considered an indicator of hemodynamic impairment. However, our study indicates that patients with high-grade ICA stenosis could remain asymptomatic despite exhibiting flow alterations. These findings suggest that changes in flow territory may occur before CBF deficits manifest, and adequate compensating collateral flow may protect patients from the deterioration of clinical symptoms. Flow assessment by rVE-ASL can demonstrate the redistribution of CBF from the contralateral ICA and VBA, reflecting compensating patterns and the presence of collateral pathways in patients with ICAD, and may help predict the borderzone prone to infarction. Importantly, rVE-ASL offers several advantages, such as noninvasive imaging without radiation exposure, no requirement for additional contrast agents, and high compatibility with other routine MR imaging (eg, DWI). Therefore, rVE-ASL can be a valuable tool for longitudinal monitoring of disease progression in patients with ICAD and may assist in decision-making regarding patient selection for interventional therapy.

This study has limitations. First, this is a pilot study with limited sample size, which may affect the generalizability of the results. Future studies with larger cohorts are needed to further validate the clinical utility of the rVE-ASL method. Second, some secondary collateral pathways, such as the ECA via the ophthalmic artery, were not evaluated in our study. However, such secondary collaterals generally develop only in patients with near-total occlusion or total occlusion of ICA when primary collaterals are insufficient. There were 4 patients who showed secondary collateral pathways developed from the ECA via the ophthalmic artery on DSA in our study. Flow territories of the ECA were successfully detected by rVE-ASL. One representative case is shown in Online Supplemental Data. Third, the number of symptomatic patients with ICA stenosis of 50%–90% was relatively small, potentially introducing some bias in the interpretation of findings. Finally, prospective studies are still warranted to investigate the prognostic effect of compensating patterns in patients with ICAD, which could be helpful in guiding patient selection for interventional therapy.

CONCLUSIONS

Our study demonstrates the feasibility of using rVE-ASL to assess collateral flows in patients with ICAD, yielding results comparable to DSA. Patients with very high-grade ICA stenosis (≥90%) are prone to exhibit flow alterations. The collateral flow in the territory of MCA on the affected side is primarily developed from the contralateral ICA, and its presence could serve as a potential predictor of symptomatic ICAD. These findings emphasize the potential clinical utility of rVE-ASL in assessing collateral circulation and its possible role in predicting and managing ICAD.

Disclosure forms provided by the authors are available with the full text and PDF of this article at www.ajnr.org.

REFERENCES

1. Liebeskind DS. **Collateral circulation.** *Stroke* 2003;34:2279–84 CrossRef Medline
2. Hartkamp NS, Petersen ET, Chappell MA, et al. **Relationship between haemodynamic impairment and collateral blood flow in carotid artery disease.** *J Cereb Blood Flow Metab* 2018;38:2021–32 CrossRef Medline
3. Vernieri F, Pasqualetti P, Matteis M, et al. **Effect of collateral blood flow and cerebral vasomotor reactivity on the outcome of carotid artery occlusion.** *Stroke* 2001;32:1552–58 CrossRef Medline
4. Hofmeijer J, Klijn CJ, Kappelle LJ, et al. **Collateral circulation via the ophthalmic artery or leptomeningeal vessels is associated with impaired cerebral vasoreactivity in patients with symptomatic carotid artery occlusion.** *Cerebrovasc Dis* 2002;14:22–26 CrossRef Medline
5. Henderson RD, Eliasziw M, Fox AJ, et al. **Angiographically defined collateral circulation and risk of stroke in patients with severe carotid artery stenosis. North American Symptomatic Carotid Endarterectomy Trial (NASCET) Group.** *Stroke* 2000;31:128–32 CrossRef Medline
6. Kaufmann TJ, Huston J 3rd, Mandrekar JN, et al. **Complications of diagnostic cerebral angiography: evaluation of 19,826 consecutive patients.** *Radiology* 2007;243:812–19 CrossRef Medline
7. Petersen ET, Zimine I, Ho YC, et al. **Non-invasive measurement of perfusion: a critical review of arterial spin labelling techniques.** *Br J Radiol* 2006;79:688–701 CrossRef Medline
8. Alsop DC, Detre JA, Golay X, et al. **Recommended implementation of arterial spin-labeled perfusion MRI for clinical applications: a consensus of the ISMRM perfusion study group and the European consortium for ASL in dementia.** *Magn Reson Med* 2015;73:102–16 CrossRef Medline
9. Detre JA, Leigh JS, Williams DS, et al. **Perfusion imaging.** *Magn Reson Med* 1992;23:37–45 CrossRef Medline
10. Williams DS, Detre JA, Leigh JS, et al. **Magnetic resonance imaging of perfusion using spin inversion of arterial water.** *Proc Natl Acad Sci USA* 1992;89:212–16 CrossRef Medline
11. Zhang X, Ghariq E, Hartkamp NS, et al. **Fast cerebral flow territory mapping using vessel encoded dynamic arterial spin labeling (VEDASL).** *Magn Reson Med* 2016;75:2041–49 CrossRef Medline
12. Wong EC. **Vessel-encoded arterial spin-labeling using pseudocontinuous tagging.** *Magn Reson Med* 2007;58:1086–91 CrossRef Medline
13. Wong EC, Guo J. **Blind detection of vascular sources and territories using random vessel encoded arterial spin labeling.** *Magn Reson Mater Phy* 2012;25:95–101 CrossRef Medline
14. Dai W, Robson PM, Shankaranarayanan A, et al. **Modified pulsed continuous arterial spin labeling for labeling of a single artery.** *Magn Reson Med* 2010;64:975–82 CrossRef Medline
15. Helle M, Norris DG, Rufer S, et al. **Superselective pseudocontinuous arterial spin labeling.** *Magn Reson Med* 2010;64:777–86 CrossRef Medline
16. van Osch MJ, Teeuwisse WM, Chen Z, et al. **Advances in arterial spin labelling MRI methods for measuring perfusion and collateral flow.** *J Cereb Blood Flow Metab* 2018;38:1461–80 CrossRef Medline
17. Okell TW, Garcia M, Chappell MA, et al. **Visualizing artery-specific blood flow patterns above the circle of Willis with vessel-encoded arterial spin labeling.** *Magn Reson Med* 2019;81:1595–604 CrossRef Medline
18. Okell TW, Harston GW, Chappell MA, et al. **Measurement of collateral perfusion in acute stroke: a vessel-encoded arterial spin labeling study.** *Sci Rep* 2019;9:8181 CrossRef Medline
19. Zhang X, Cao YZ, Mu XH, et al. **Highly accelerated compressed sensing time-of-flight magnetic resonance angiography may be reliable for diagnosing head and neck arterial steno-occlusive disease: a comparative study with digital subtraction angiography.** *Eur Radiol* 2020;30:3059–65 CrossRef Medline
20. North American Symptomatic Carotid Endarterectomy Trial. **Methods, patient characteristics, and progress.** *Stroke* 1991;22:711–20 CrossRef Medline
21. van Laar PJ, Hendrikse J, Klijn CJ, et al. **Symptomatic carotid artery occlusion: flow territories of major brain-feeding arteries.** *Radiology* 2007;242:526–34 CrossRef Medline
22. Rutgers DR, Klijn CJ, Kappelle LJ, et al. **A longitudinal study of collateral flow patterns in the circle of Willis and the ophthalmic artery in patients with a symptomatic internal carotid artery occlusion.** *Stroke* 2000;31:1913–20 CrossRef Medline
23. Chng SM, Petersen ET, Zimine I, et al. **Territorial arterial spin labeling in the assessment of collateral circulation: comparison with digital subtraction angiography.** *Stroke* 2008;39:3248–54 CrossRef Medline
24. Arteaga DF, Strother MK, Davis LT, et al. **Planning-free cerebral blood flow territory mapping in patients with intracranial arterial stenosis.** *J Cereb Blood Flow Metab* 2017;37:1944–58 CrossRef Medline
25. Kluytmans M, van der Grond J, van Everdingen KJ, et al. **Cerebral hemodynamics in relation to patterns of collateral flow.** *Stroke* 1999;30:1432–39 CrossRef Medline
26. Hendrikse J, Hartkamp MJ, Hillen B, et al. **Collateral ability of the circle of Willis in patients with unilateral internal carotid artery occlusion: border zone infarcts and clinical symptoms.** *Stroke* 2001;32:2768–73 CrossRef Medline
27. Hoksbergen AW, Majoie CB, Hulsmans FJ, et al. **Assessment of the collateral function of the circle of Willis: three-dimensional time-of-flight MR angiography compared with transcranial color-coded duplex sonography.** *AJNR Am J Neuroradiol* 2003;24:456–62 Medline
28. Lee JH, Choi CG, Kim DK, et al. **Relationship between circle of Willis morphology on 3D time-of-flight MR angiograms and transient ischemia during vascular clamping of the internal carotid artery during carotid endarterectomy.** *AJNR Am J Neuroradiol* 2004;25:558–64 Medline
29. Fang H, Song B, Cheng B, et al. **Compensatory patterns of collateral flow in stroke patients with unilateral and bilateral carotid stenosis.** *BMC Neurol* 2016;16:39 CrossRef Medline
30. Chen YF, Tang SC, Wu WC, et al. **Alterations of cerebral perfusion in asymptomatic internal carotid artery steno-occlusive disease.** *Sci Rep* 2017;7:1841 CrossRef Medline